Regenerative Engineering and Translational Medicine (2018) 4:154–161
https://doi.org/10.1007/s40883-018-0057-z

Nanofibrous Nerve Conduits with Pre-seeded Bone Marrow Stromal Cells and Cultured by Bioreactor for Enhancing Peripheral Nerve Regeneration

Gan Zhou[1] · Wei Chang[1] · Xiaojun Yu[1]

Received: 29 January 2018 / Accepted: 27 April 2018 / Published online: 11 May 2018

Abstract

Peripheral nerve injury (PNI) remains one of the most common causes of disability or loss of sensations. Schwann cells (SCs) seeded synthetic nerve conduits have been widely studied for treating PNI. However, this approach is limited by poor accessibility of SCs and lack of dominance by seeded cells. In this study, a novel polycaprolactone (PCL)-based nerve conduit was seeded with bone marrow stromal cells (BMSCs), and the cells were differentiated into Schwann cell-like cells (BMSC-SCs) as a replacement for SCs. The influences of initial cell seeding density on cell proliferation were evaluated. A rotary cell culture system (RCCS) was adopted to dynamically culture the BMSCs seeded on PCL nerve conduits to further improve cell proliferation, differentiation, and neurite extension. The initial cell seeding density of 1×10^5 cells per conduit resulted in the highest proliferation of BMSCs on the PCL nerve conduits. Based on the results of MTS and RT-qPCR, substantial improvements in the proliferation and differentiation of BMSCs were achieved by culturing the BMSCs pre-seeded on PCL nerve conduits in RCCS at the rotating speed of 16 rpm. The neurite outgrowth from PC12 cells was significantly enhanced on nerve conduits pre-seeded with BMSCs and pre-cultured in RCCS. This study demonstrated that dynamic culturing condition provided a better environment for the proliferation and differentiation of BMSCs on novel PCL nerve conduits than that of the static culturing condition. The combination of PCL nerve conduit, BMSCs, and dynamic culture in RCCS could be potentially used as an alternative solution to treat PNI.

Lay Summary

Peripheral nerve injury (PNI) is one of the leading cause of disabilities. Therapeutic strategies involving cell transplantation showed great promise from previous studies. However, the lack of a reliable cell source and poor culture condition compromise the healing outcome. In this study, a novel polymer-based nerve conduit was seeded with bone marrow stromal cells (BMSCs) and cultured with a rotary cell culture system (RCCS). The influences of initial cell seeding density and the rotating speed of RCCS were investigated. The results indicated that the proliferation and differentiation of BMSCs on nerve conduits were significantly increased in the RCCS with the rotating speed of 16 rpm. The neurite outgrowth from PC12 cells was significantly enhanced on the nerve conduits pre-seeded with BMSCs and pre-cultured in RCCS. This new strategy could potentially be a promising treatment for PNI.

In the future, the nerve conduits could be further modified by incorporation of extracellular matrix proteins and growth factors. Moreover, the in vivo animal studies are needed for evaluating the efficacy of the nerve conduits for the treatment of PNI.

Keywords Peripheral nerve · Bone marrow stromal cells · Bioreactor · Stem cell · Differentiation

Introduction

Peripheral nerve injuries (PNI) have become one of the most common mechanical traumas which can be caused by car accident or gunshot, and untreated PNI will lead to disabilities or sensation loss of injured site after injury [1]. The neurons of peripheral nervous system (PNS) has intrinsic ability to regenerate injured axons. However, this self-regeneration is greatly compromised with the increase of nerve injury gap length, especially when the gap length is greater than 4–5 mm [2]. Autograft remains the golden standard for the treatment of PNI [3]. However, the autograft approach is plagued by the limited availability and donor site mobility. In recent decades, more artificial nerve conduits are used to bridge the nerve injury gap

✉ Xiaojun Yu
xyu@stevens.edu

[1] Department of Biomedical Engineering, Chemistry and Biological Sciences, Stevens Institute of Technology, Hoboken, NJ, USA

that exceed 4 mm [2]. Despite the improvements on artificial nerve conduits were achieved, they are still limited by sub-optimal conduit structure, the lack of guidance to regenerated tissue, the lack of chemical and physical support from Schwann cells, and misconnection of axon [4, 5]. Therefore, fully functional recovery for large nerve gap is always hard to accomplish, and it is still challenging to develop novel nerve conduits for repairing peripheral nerve injuries [6].

The cell therapy to treat PNI with Schwann cells has been reported previously, and various successes have been achieved [7]. Because the applications of autologous Schwann cells are limited by poor cell accessibility, inability to harvest in large mount quickly, and dysfunction on donor site [8], alternative cell sources have been reported by other researches [9]. In order to replace Schwann cells in cell therapy for PNI, protocols for in vitro cell differentiation from Bone marrow stromal cells (BMSCs) to Schwann cell-like cells have been developed [9, 10]. Accumulating evidence showed that a cocktail of growth factors such as platelet derived growth factor (PDGF), forskolin, basic fibroblast growth factor (bFGF), and β-heregulin could lead to phenotype change from BMSC to Schwann cell-like cells (SC-Cs) when added into growth medium of BMSCs [11]. The change in phenotype was confirmed by variation in gene and protein expression level, and bone marrow stromal cell-derived Schwann cell-like cells (BMSC-SCs) showed great potential in treating PNI [12].

Previously, a few nerve conduits have been developed to substitute autograft, with the goal to promote cell attachment and proliferation. For instance, an electrospun nerve guidance conduit using a blend of polyurea and polycaprolactone was developed to provide both biochemical and topographical cues for human neural stem cells (hNSCs) [13]. However, due to the limitation by the synthesis method, the nerve conduit can only achieve 200–500 μm channels which are not comparable with the native topography of peripheral nerve. An electrospun silk fibroin nerve conduit was fabricated to bridge rat sciatic nerve defect [14]. However, due to the lack of inner surface for cell attachment, the regeneration results were dissatisfied.

The initial cell seeding density was shown to be critical in cell therapy [15], as it can greatly influence cell proliferation [16], alignment [17], and differentiation [18, 19]. BMSCs were reported to yield a higher endogenous osteogenic signal expression and better mineralization when cultured with optimal seeding density in bone reconstitution [14–18]. However, the impact of initial seeding density on proliferation and neurogenic differentiation of BMSCs reminds unclear. The optimal initial seeding density for the PCL nerve guide conduit needs to be determined.

The improvement of proliferation and differentiation for cells seeded on three-dimensional (3-D) nerve conduit requires enhanced fluid flow and nutrient/waste exchange, which could be facilitated through the use of Rotary Cell Culture System (RCCS) [20, 21]. RCCS was demonstrated to be a helpful cell culture tool in tissue engineering [22, 23]. Through continuous rotation of the culture vessel, a dynamic fluid flow culture environment was created for improving cell proliferation and differentiation [24]. RCCS could be used in development of nerve tissue in vitro, given that they can provide fluid dynamic and physical regulatory signals similar to in vivo environment for promoting cell proliferation, differentiation, and ECM production [25]. As shown in previous studies, RCCS was used to promote neural stem cell differentiation to achieve nerve-like tissue construction in vitro [26]. Also, it was used to promote the cardiomyogenic differentiation of embryonic stem cells in vitro [27]. These studies confirmed the positive role of RCCS on nerve tissue growth and cell differentiation. The laminar flow and physical support produced by RCCS were directly related to its rotatory speed [28]. As in most of the previous studies, the carrier of cells inside RCCS was usually microbeads and the RCCS was set to a fixed rotation speed [24]. However, less attention was drawn on the influence of RCCS rotatory speed on the proliferation and differentiation of cells seeded on nerve conduits. It is necessary to investigate the influences of rotatory speed of RCCS on the proliferation and differentiation of BMSCs seeded on PCL nerve conduits.

In this study, we investigated the influence of cell seeding density and rotatory speed of RCCS on the proliferation and differentiation of BMSCs seeded novel PCL nerve conduits, and the capability of the nerve conduits pre-seeded with BMSCs and pre-cultured in RCCS to promote neurite extension in vitro. Scanning electron microscope (SEM) was used to characterize the morphology of the PCL nerve conduits. MTS assay and immunostaining technique were used to access cell proliferation, alignment, and infiltration into the conduits. Immunofluorescence staining and RT-qPCR were used to evaluate the differentiation of BMSCs into Schwann cell-like cells on nerve conduits. The PC12 cells were cultured on PCL nerve conduits pre-seeded with BMSCs and pre-cultured in RCCS in order to evaluate the efficacy of the nerve conduits to promote neurite extension in vitro.

Materials and Methods

PCL Nerve Guide Conduits Construction

A glass Petri dish (d = 10 cm) was cleaned, and 500 μl of 20% (w/v) glucose was added into the Petri dish to cover the whole bottom by smeared uniformly. The glass Petri dish was then heated in an oven at 65 °C for 10 min, and salt particles (size between 101 and 150 μm) were poured onto the bottom of the Petri dish to cover the whole bottom surface. Afterwards, Petri dish was put into an oven (65 °C) for 30 s, and the extra salt

was removed. The solution of 4 ml of 8% (*w*/*v*) PCL (Sigma) in DCM was poured onto the Petri dish to cover the whole bottom. After the solution was dried thoroughly, the Petri dish was soaked into DI water, and the PCL sheet was detached. The collected PCL sheet was cut into 17 mm × 11 mm pieces and rolled into spiral structured conduits with the final diameter of 1.6 to 1.8 mm.

Unidirectional aligned PCL nanofibers were fabricated on the inner surface of PCL nerve conduits by electrospinning 16% (*w*/*v*) PCL onto a high-speed rotating metal disc. Briefly, 16% (*w*/*v*) PCL solution was prepared by dissolving PCL (Sigma) in 1,1,1,3,3,3-hexafluoro-2-propanol (HFIP) under room temperature (RT). After fully dissolved, the PCL solution was loaded into a 5-ml syringe and released at a flow rate of 0.25 ml/h through a 19 gauge blunt head needle that connected to a high-voltage power source. Under a high voltage (10–11 kV), the PCL nanofibers were electrospun and collected onto the surface of PCL sheet that was fixed onto a customer designed spinning disc, while the disc was spinning at 975 rpm. After 10 min of electrospinning, the PCL sheet was covered by PCL nanofibers. The excessive fibers were removed, and the PCL sheets were rolled into spiral structured conduits. The PCL conduits were lined uni-axially on an iron wire for electrospinning the outer fibers. The outer fibers were electrospun with the same PCL solution and the same electrospinning setup for 16 min.

Bone Marrow Stromal Cell Culture

The tibia and femur of young male Sprague-Dawley rats (250–300 g) were used to isolate bone marrows, and BMSCs were harvested according to previous protocol [29]. Briefly, the animals were sacrificed by using an overdose of CO_2 asphyxiation. Bone marrow cavity contents were removed by washing with Dulbecco's modified Eagle's medium (DMEM) with 10% (*v*/*v*) FBS, 1% (*v*/*v*) penicillin. The bone marrows were passed through 16 and 20 gauge needles, centrifuged and re-suspended in fresh medium and transferred into a T-75 cell culture flask with 10 ml of Dulbecco's modified Eagle's medium (DMEM) with 10% (*v*/*v*) FBS, 1% (*v*/*v*) penicillin. Once the cells reached confluence, the cells were trypsinized and seeded onto the nerve conduits according to desired initial cell seeding density.

BMSC-SC Induction In Vitro

BMSCs were cultured in cell induction medium, composed of Dulbecco's modified Eagle's medium (DMEM) with 5% (*v*/*v*) FBS, β-heregulin 100 ng/ml, platelet-derived growth factor-AA 5 ng/ml, Forskolin 5 μM, and basic fibroblast growth factor 10 ng/ml, for 21 days. The medium was changed every other day.

Cell Proliferation Test

To measure cell proliferation and viability, at days 1, 7, 14, and 21 ($n = 5$), MTS (3-(4,5-dimethylthiazol-2-yl)-5-(3-carboxymethoxyphenyl)-2-(4-sulfophenyl)-2htetrazolium) assay (Promega, Madison, WI) was used according to previous protocol [29]. Comparisons were made between different cell seeding densities and different rotation speeds for RCCS.

Quantification of Gene Expression

Gene expression was assessed using reverse transcriptase quantitative polymerase chain reaction (RT-qPCR). At day 21, RNA was extracted from the samples from three different seeding densities (1×10^4, 5×10^4, and 1×10^5 cells per conduit), three different rotating speeds (16, 24, and 32 rpm) and the control group by using a Qiagen RNA MiniPrep Kit (Qiagen, Netherlands). RNA concentration was determined by an ND-1000 spectrophotometer ($n = 4$) (Nanodrop, Wilmington, DE), and 5 ng of RNA was applied in RT-qPCR according to the manufacturer's instructions. Primers specific for Nuregulin-1 (Nrg-1) were designed according to *Power SYBR® Green RNA-to-CT™ 1-Step Kit Protocol* provided by the manufacturer, and the whole quantification-PCR was performed as the manufacturer suggested.

Immunocytochemistry

At day 21, samples from every conditions were rinsed and then fixed with 4% paraformaldehyde, overnight at 4 °C. After fixation, all samples were rinsed with Tris-buffered saline solution with 1% tween (TBST). Samples were then blocked by 5% (*w*/*v*) bovine serum albumin (BSA) in TBST at room temperature for 45 min. Afterwards, the samples were rinsed once with PBS and incubated in 1:100 rabbit polyclonal anti-S-100 (Sigma, St. Louis, MO) in TBST with 5% BSA at 4 °C overnight. After primary antibody incubation, all samples were rinsed three times with TBST, 10 min each, and incubated with 1:300 Alexa Fluor ® 488 Goat anti-rabbit IgG (Life Technologies, Norwalk, CT) in 5% BSA in TBST at room temperature for 1.5 h. After secondary antibody incubation, all samples were rinsed three times with TBST for 10 min. Then, DAPI (Sigma, St. Louis, MO) was added onto the samples to stain the nucleate. All images were taken at ×20 with a Zeiss Pascal LSM 5 confocal microscope (Germany).

Optimal Cell Seeding Density

After reaching confluence, the BMSCs were seeded onto nerve conduits at densities of 1×10^4 cells/conduit, 5×10^4 cells/conduit, and 1×10^5 cells/conduit ($n = 6$), and nerve conduits were placed in 24-well tissue culture plates (TCP). Cell proliferation and differentiation were accessed to determine

the optimal cell seeding density. The cells were seeded onto TCP at the density of 5×10^4 cells/well as the control. All medium was changed every other day.

Optimal RCCS Rotating Speed

After the optimal cell seeding density was determined, the BMSCs were seeded onto nerve conduits at the optimal seeding density ($n = 6$), and the nerve conduits were placed in 24-well tissue culture plate (TCP) and cultured with cell induction medium (TCP group). The nerve conduits were cultured in RCCS with rotating speeds of 16, 24, and 32 rpm separately (RCCS groups). Cell proliferation and differentiation were accessed to determine the optimal rotating speed. BMSCs were seeded at 5×10^4 cells/well ($n = 6$) into TCP and cultured with complete medium as a control group. All medium was changed every other day.

Co-culture of Schwann Cell-Like Cells with PC12 Cells

Nerve conduits seeded with BMSCs were cultured in RCCS with optimal rotating speed and differentiation medium for 21 days. At day 21, PC12 cells with the number of 300–500 were seeded onto the nerve conduits cluster per conduit. After PC12 cells were seeded, PC12 cell differentiation medium, composed of RPMI with 10% (*v*/*v*) horse serum, 5% FBS (*v*/*v*) and 1% (*v*/*v*) penicillin, and with 50 ng/ml NGF, was used for co-culture. The medium was changed every day and fresh NGF was added when changing the medium. The co-culture lasted 10 days before all samples were collected and fixed with 4% (*w*/*v*) paraformaldehyde.

Samples of co-culture of Schwann cell-like cells with PC12 cells were immunostained with the similar technique as described in the immunocytochemistry section. Samples were fixed with 4% paraformaldehyde and rinsed with Tris-buffered saline solution with 1% tween (TBST). Samples were then blocked by 5% (*w*/*v*) bovine serum albumin (BSA) in TBST at room temperature for 45 min. Afterwards, the samples were rinsed once with PBS and incubated in 1:100 mouse monoclonal anti-neurofilament (Thermo Fisher Scientific) in TBST with 5% BSA at 4 °C overnight. After primary antibody incubation, all samples were rinsed three times with TBST for 10 min and incubated with 1:300 Alexa Fluor ® 488 Donkey Anti-Mouse IgG (Life Technologies, Norwalk, CT) in 5% BSA in TBST at room temperature for 1.5 h. After secondary antibody incubation, all samples were rinsed three times with TBST for 10 min. Then, DAPI (Sigma, St. Louis, MO) was added onto the samples to stain the nucleate. All image was taken at ×20 with a Zeiss Pascal LSM 5 confocal microscope (Germany).

Results

The SEM was used to observe the morphology of the PCL nerve conduits. As shown in Fig. 1a, b, the PCL sheet was rolled into a spiral conduit, with the inner side of the conduit covered by aligned fibers and the outer surface covered by random fibers. Figure 1c shows the pores with a size range of 100–150 μm, which was formed throughout the PCL sheet by leaching of salt particles. After electrospinning, the inner surface of the nerve conduits was covered by aligned fibers as shown in Fig. 1d, and the direction of the fiber followed the longitude of the conduit (data not shown). These observations confirmed the formation of pores, fibers, and inner structures in the PCL nerve conduits.

In order to determine optimal seeding density and rotating speed, MTS was performed at day 1, day 7, day 14, and day 21 during cell culture period. As shown in Fig. 2, there was significant difference ($P = 5.8E\text{-}05$) in cell number between each seeding density ($n = 6$) at day 21. Compared to day 1, all groups had significant increase in cell numbers after 21 days of culture, and the group with cell seeding density of 1×10^5 cells/conduit showed the highest living cell number and highest proliferation rate. As observed from day 14 to day 21, all groups with differentiation medium showed a lag of proliferation, and it was the sign for indicating the beginning of cell differentiation as suggested by previous research. According to the MTS results, the cell seeding density of 1×10^5 cells/conduit was determined to be the optimal cell seeding density.

After the optimal seeding density was determined, the nerve conduits were seeded with 1×10^5 cells/conduit ($n = 6$) and cultured in RCCS with different rotating speeds of 16, 24, and 32 rpm. In order to determine optimal rotating speed, MTS was performed at day 1, day 7, day 14, and day 21 during cell culture period. As shown in Fig. 3, there were significant differences ($P = 0.041$) in cell number among the groups with different rotation speeds. Compared to day 1, all groups had significant increase in cell numbers after 21 days of culture, and the group with rotating speed of 16 rpm showed the highest living cell number and highest proliferation rate. According to these MTS results, the rotating speed of 16 rpm was determined to be the optimal rotating speed for RCCS.

The expression level of Neuregulin-1 was quantitatively analyzed by RT-qPCR (Fig. 4). Because no differentiation was observed on earlier time point (data not shown), the expression of Nrg-1 on day 14 and day 21 for each group was analyzed through RT-qPCR. In comparison to the control group, Nrg-1 expression level had a significant increase in all groups cultured with differentiation medium, which confirmed the induction of differentiation from BMSC to BMSC-SC. Significant difference ($P = 0.0108$) among groups with different RCCS rotation speeds was observed. The highest Nrg-1 expression level appeared in the group with rotating speed of 16 rpm, which confirmed that RCCS was helpful in

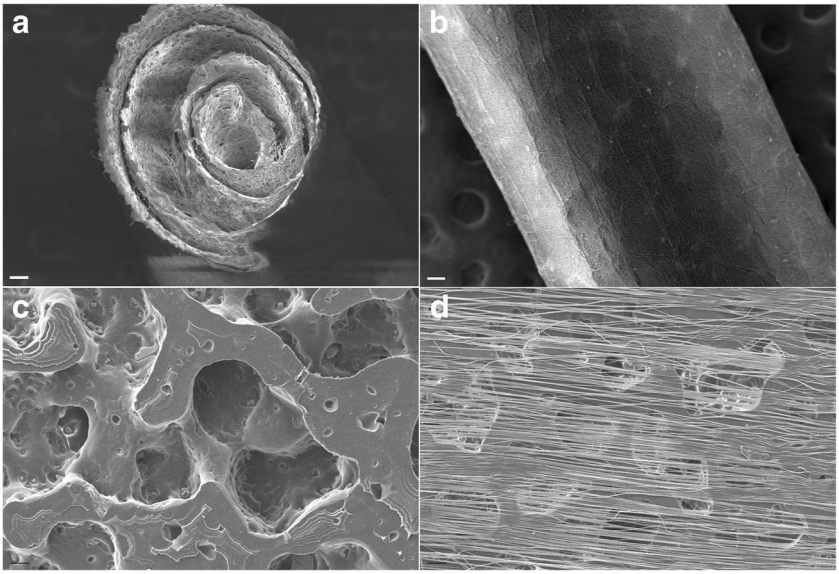

Fig. 1 **a** The cross section of PCL nerve conduit, scale bar 100 μm. **b** The outer surface of PCL nerve conduit, scale bar 100 μm. **c** Pores on PCL sheet before electrospinning, scale bar 20 μm. **d** Pores on PCL sheet after electrospinning, scale bar 100 μm

promoting cell differentiation. Moreover, the difference in Nrg-1 expression level suggested that the BMSC-SCs on the nerve conduits in the RCCS with rotating speed of 16 rpm had better maturation and myelination.

Protein expression level and cell proliferation were visualized by immunofluorescence staining and imaging. As shown in Fig. 5, S-100 was immunostained with Anti-S-100 antibody, and the staining illustrated visible S-100 expression difference between each sample at day 21. From Fig. 5, the cell bodies of BMSC-SCs were regulated by aligned fibers. The group with initial cell seeding density of 1×10^5 cell/conduit showed the highest cell coverage on the surface of nerve conduits, which further confirmed that the cell seeding density of 1×10^5 cell/conduit was the optimal cell seeding density. Moreover, difference on cell number was noticed among the groups with different RCCS rotary speeds, which also confirmed that the 16 rpm was the optimal rotary speed. Figure 6 clearly shows the difference in the thickness of cell layers between static culture group and RCCS groups, which confirmed the role of bioreactor in promoting cell infiltration and proliferation.

Neurite extension was accessed by immunostaining of neurofilament and measurement of neurite length through visualization by using the confocal microscope. As shown in Fig. 7, the RSSC group cultured in medium with NGF had the longest neurite extension. Significant difference ($P = 1.26E-08$) in neurite length was shown between the static culture group with NGF and the group without NGF.

Discussion

The purpose of this study was to use RCCS to promote the differentiation of BMSCs seeded on nerve conduits into BMSC-SCs and to investigate the influence of initial cell seeding density and RCCS rotary speed on the proliferation and differentiation of cells on nerve conduits for peripheral nerve regeneration.

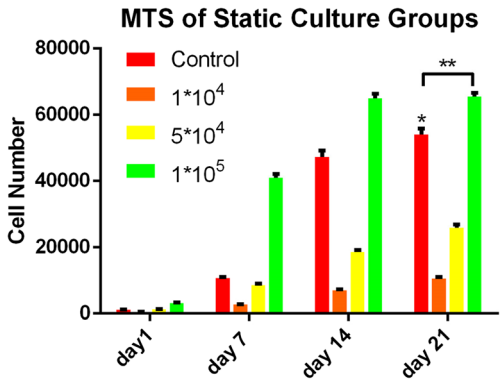

Fig. 2 MTS results of Static Culture Groups with different cell seeding densities. *Significant difference ($P = 0.0434$) between 5×10^4 and control group. **Significant difference ($P = 5.8E-05$) between 1×10^5 and other cell seeding densities

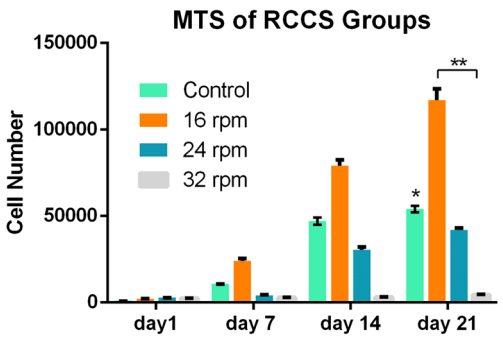

Fig. 3 MTS results of RCCS group with different rotation speeds. *Significant difference ($P = 0.001$) between each rotating speed and control group. **Significant difference ($P = 0.041$) between 16 rpm and other rotating speeds

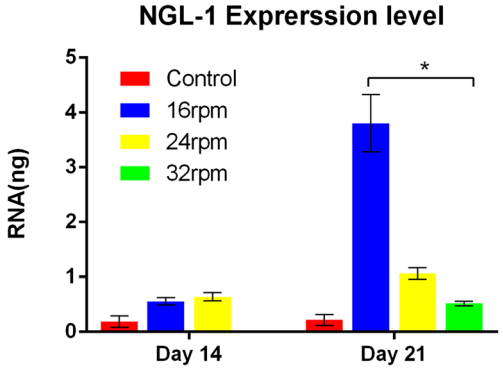

Fig. 4 Expression level of Nrg-1 of all groups that quantified by RT-qPCR. *Significant difference ($P = 0.0108$) between different rotating speed

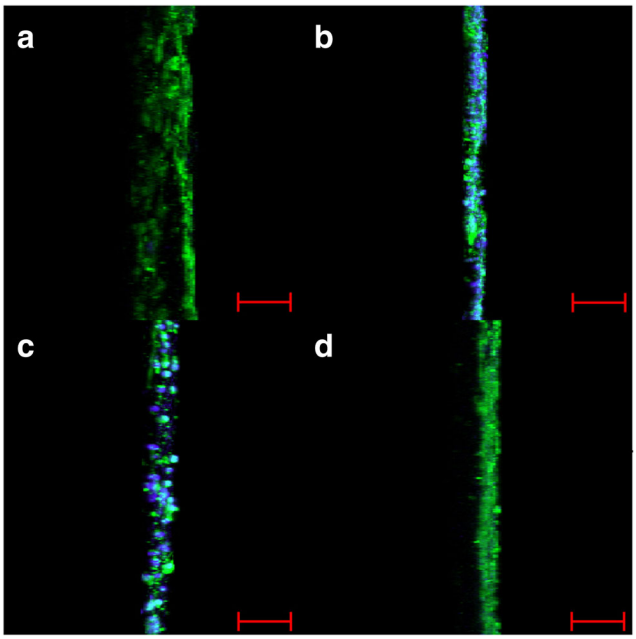

Fig. 6 Immunofluorescence images of the Z-stack (view from side) of PCL nerve conduits of all RSSC groups and control group. **a** 16 rpm. **b** 24 rpm. **c** 32 rpm. **d** Control group. The scale bars are 100 μm

As reported in the previous study, cell attachment reached a peak at the pore size around 120 μm [30], which is consistent with our previous research for optimizing pore size for PCL nerve conduits [31]. The nerve conduit was fabricated into 17 mm in length and 1.6–1.8 mm in diameter in order to be consistent with the following in vivo study for evaluating the nerve conduit in bridging a 15 mm long sciatic nerve defect in a rat model with the diameter of rat sciatic nerve around 1.6 mm [32]. Therefore, the nerve conduit was fabricated to be 17 mm in length in order to create a 15-mm gap length and an extra 1 mm chamber on both ends of the conduit to hold the nerve stumps. Meanwhile, the diameter of the nerve conduit was set to be 1.6 to 1.8 mm in order to properly fit the nerve stumps. Aligned PCL nanofibers were electrospun on the conduit in order to mimic the natural alignment of fibrin cable and guide the migration of BMSCs after nerve injury. The fiber

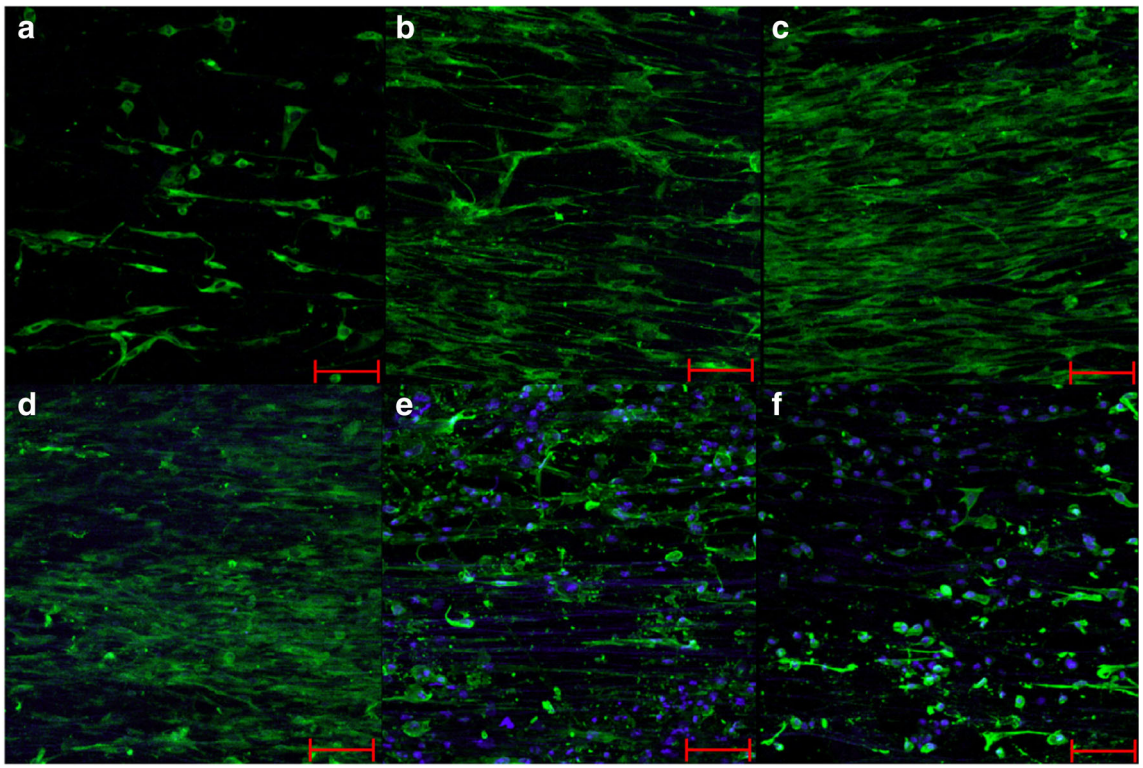

Fig. 5 Immunofluorescence images of the surface of PCL nerve conduit of all groups. **a** 1×10^4 cells per conduit. **b** 5×10^4 cells per conduit. **c** 1×10^5 cells per conduit. **d** 16 rpm. **e** 24 rpm. **f** 32 rpm. The scale bars are 100 μm

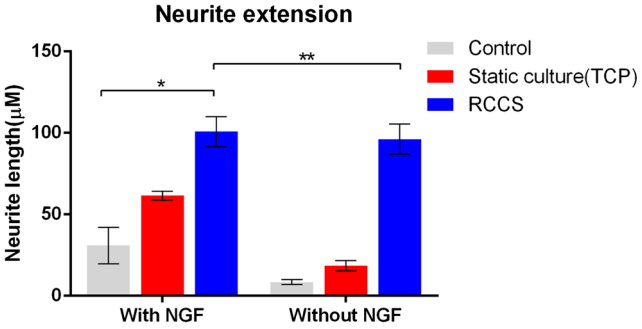

Fig. 7 Length of PC12 neurite extension of control, static culture, and RCCS groups when cultured with or without NGF. *Significant difference ($P = 1.26E-08$) between each culture method. **Significant difference ($P = 0.18$) between groups with NGF and without NGF

diameter and fiber density will be influenced by electrospinning parameters and time. As previously reported by our lab [31, 33], the electrospinning parameters and time were optimized to achieve preferred fiber diameter and fiber coverage. The material properties of the spiral scaffolds were characterized previously based on the Young's Modulus, the Yield Strength, the porosity, and the surface area to volume ratio [31, 33]. The data indicated that the properties of the scaffolds were matching with those of native nerve tissues, and thus the nerve conduits were suitable for repairing peripheral nerve injuries [31].

Due to the morphological and biological differences between synthesized nerve conduit and nerve tissue, cell attachment was greatly compromised. The surface of spiral nerve conduit was functionalized by depositing aligned PCL nanofibers to increase surface areas and provide extracellular matrix mimics to improve initial cell attachment [29, 31].

The initial cell seeding density and RCCS rotating speed were optimized to enhance cell proliferation and differentiation. As shown in Fig. 2, the cell seeding density of 1×10^5 cells/conduit showed the highest cell proliferation at days 7, 14, and 21 among all the experimental groups, and thus, the seeding density of 1×10^5 cells per conduit was determined to be the optimal initial cell seeding density. It had been reported that further increasing initial cell seeding densities did not yield better proliferation and differentiation of cells [15]. Therefore, higher initial cell seeding density than that of 1×10^5 cells per conduit was not adopted in the current study.

As shown in Figs. 3 and 5, the cell number of the 16 rpm group in RCCS was significantly higher as compared to that of static culture group and the other groups in RCCS, and thus, the 16 rpm was determined to be the optimal rotating speed for promoting the BMSCs seeded on nerve conduits in RCCS. The dynamic culture condition in RCCS at 16 rpm enhanced the fluid flow transport and improved nutrient supply to cells, and thus promoted cell proliferation. However, the cell number in 32 rpm group was significantly less than the other groups throughout culture period of 21 days. This could be due to the fact that shear force created within RCCS while it was rotating at 32 rpm was too strong for cells to grow and thus the environment was not suitable for the proliferation of cells [34]. Both MTS results and immunofluorescence images were consistent with the conclusion that higher rotating speed such as 24 and 32 rpm in dynamic culture conditions led to reduce proliferation of cells on nerve conduits in RCCS as compared to static culture conditions.

RT-qPCR was used to quantitatively analyze the gene expression level of Nrg-1 which was indicated as a critical biomarker for the survival and maturation of SCs [35]. The rotary speed of RCCS could influence not only cell proliferation but also cell differentiation. As shown in Fig. 4, the Nrg-1 expression was significantly upregulated at the rotating speed of 16 rpm in RCCS.

Observations from immunofluorescence images suggested that aligned PCL fibers on nerve conduits could guide the orientation of BMSCs towards the same direction, and a thicker cell layer was formed on the nerve conduits in RCCS (Fig. 6). These observations were consistent with MTS and RT-qPCR results and are consistent with our previous research [29, 31].

In order to evaluate the efficacy of the nerve conduits for peripheral nerve regeneration, the PC12 cells were cultured on nerve conduits pre-seeded with BMSCs and pre-cultured in RCCs, and the neurite outgrowth from PC12 cells was characterized. The results indicated that the combination of PCL nerve conduits, BMSCs, and dynamic culture in RCCS significantly enhanced neurite extension from PC12 cells (Fig. 7). Nerve growth factor (NGF) was needed by PC12 cells for neurite extension. As shown in Fig. 7, no significant difference ($P = 0.18$) was observed between the RCCS group with NGF and the group without NGF, which indicated that BMSCs had the capability to secrete NGF to promote neurite outgrowth from PC12 cells.

Conclusion

Current study demonstrated that the novel PCL nerve conduits were able to direct cell alignment and to improve cell proliferation and differentiation. MTS data suggested that the optimal cell seeding density was 1×10^5 cells/conduit, as it showed the highest cell proliferation among all the experimental groups at the culture time points of 7, 14, and 21 days. As indicated by the results from MTS and RT-qPCR, the proliferation and differentiation of BMSCs seeded on the PCL nerve conduits were significantly influenced by the dynamic culture conditions in RCCS. The proliferation and differentiation of BMSCs seeded on nerve conduits were significantly increased in the RCCS with the rotating speed of 16 rpm. The neurite outgrowth from PC12 cells was significantly enhanced on nerve conduits pre-seeded with BMSCs and pre-cultured in RCCS. These findings demonstrated that the combination of novel nerve conduit, BMSCs, and the dynamic culture in RCCS could be a promising strategy for improving peripheral nerve regeneration.

Acknowledgements The work is supported by the Stevens I&E Doctoral Fellowship Program and Office of the Assistant Secretary of Defense for Health Affairs through the Peer Reviewed Orthopedic Research Program under Award Nos. (W81XWH-13-1-0320) and (W81XWH-16-1-0132).

References

1. Noble J, Munro CA, Prasad VSSV, Midha R. Analysis of upper and lower extremity peripheral nerve injuries in a population of patients with multiple injuries. J Trauma Acute Care Surg. 1998;45(1):116–22.
2. Politis M, Ederle K, Spencer P. Tropism in nerve regeneration in vivo. Attraction of regenerating axons by diffusible factors derived from cells in distal nerve stumps of transected peripheral nerves. Brain Res. 1982;253(1):1–12.
3. Faroni A, et al. Peripheral nerve regeneration: experimental strategies and future perspectives. Adv Drug Deliv Rev. 2015;82:160–7.
4. Gao M, Lu P, Lynam D, Bednark B, Campana WM, Sakamoto J, et al. BDNF gene delivery within and beyond templated agarose multi-channel guidance scaffolds enhances peripheral nerve regeneration. J Neural Eng. 2016;13(6):066011.
5. Wu X, He L, Li W, Li H, Wong WM, Ramakrishna S, et al. Functional self-assembling peptide nanofiber hydrogel for peripheral nerve regeneration. Regen Biomater. 2017;4(1):21–30.
6. Gobrecht P, Andreadaki A, Diekmann H, Heskamp A, Leibinger M, Fischer D. Promotion of functional nerve regeneration by inhibition of microtubule detyrosination. J Neurosci. 2016;36(14):3890–902.
7. Junka R, Yu X. Novel acellular scaffold made from decellularized schwann cell sheets for peripheral nerve regeneration. Regen Eng Translat Med. 2015;1(1–4):22–31.
8. Kingham PJ, Kalbermatten DF, Mahay D, Armstrong SJ, Wiberg M, Terenghi G. Adipose-derived stem cells differentiate into a Schwann cell phenotype and promote neurite outgrowth in vitro. Exp Neurol. 2007;207(2):267–74.
9. Zhao Z, Wang Y, Peng J, Ren Z, Zhang L, Guo Q, et al. Improvement in nerve regeneration through a decellularized nerve graft by supplementation with bone marrow stromal cells in fibrin. Cell Transplant. 2014;23(1):97–110.
10. Eglitis MA, Mezey É. Hematopoietic cells differentiate into both microglia and macroglia in the brains of adult mice. Proc Natl Acad Sci. 1997;94(8):4080–5.
11. Cogle CR, Theise ND, Fu DT, Ucar D, Lee S, Guthrie SM, et al. Bone marrow contributes to epithelial cancers in mice and humans as developmental mimicry. Stem Cells. 2007;25(8):1881–7.
12. Ao Q, Fung CK, Yat-Ping Tsui A, Cai S, Zuo HC, Chan YS, et al. The regeneration of transected sciatic nerves of adult rats using chitosan nerve conduits seeded with bone marrow stromal cell-derived Schwann cells. Biomaterials. 2011;32(3):787–96.
13. Jenkins PM, Laughter MR, Lee DJ, Lee YM, Freed CR, Park D. A nerve guidance conduit with topographical and biochemical cues: potential application using human neural stem cells. Nanoscale Res Lett. 2015;10(1):264.
14. Park SY, Ki CS, Park YH, Lee KG, Kang SW, Kweon HY, et al. Functional recovery guided by an electrospun silk fibroin conduit after sciatic nerve injury in rats. J Tissue Eng Regen Med. 2015;9(1):66–76.
15. Lode A, Bernhardt A, Gelinsky M. Cultivation of human bone marrow stromal cells on three-dimensional scaffolds of mineralized collagen: influence of seeding density on colonization, proliferation and osteogenic differentiation. J Tissue Eng Regen Med. 2008;2(7):400–7.
16. Mauck R, et al. The role of cell seeding density and nutrient supply for articular cartilage tissue engineering with deformational loading. Osteoarthr Cartil. 2003;11(12):879–90.
17. Dvir-Ginzberg M, Gamlieli-Bonshtein I, Agbaria R, Cohen S. Liver tissue engineering within alginate scaffolds: effects of cell-seeding density on hepatocyte viability, morphology, and function. Tissue Eng. 2003;9(4):757–66.
18. Kim K, Dean D, Lu A, Mikos AG, Fisher JP. Early osteogenic signal expression of rat bone marrow stromal cells is influenced by both hydroxyapatite nanoparticle content and initial cell seeding density in biodegradable nanocomposite scaffolds. Acta Biomater. 2011;7(3):1249–64.
19. Hui T, et al. In vitro chondrogenic differentiation of human mesenchymal stem cells in collagen microspheres: influence of cell seeding density and collagen concentration. Biomaterials. 2008;29(22):3201–12.
20. Marsano A, et al. Bi-zonal cartilaginous tissues engineered in a rotary cell culture system. Biorheology. 2006;43(3, 4):553–60.
21. Baraniak PR, McDevitt TC. Scaffold-free culture of mesenchymal stem cell spheroids in suspension preserves multilineage potential. Cell Tissue Res. 2012;347(3):701–11.
22. Luo H, Zhu B, Zhang Y, Jin Y. Tissue-engineered nerve constructs under a microgravity system for peripheral nerve regeneration. Tissue Eng A. 2014;21(1–2):267–76.
23. Li S, Ma Z, Niu Z, Qian H, Xuan D, Hou R, et al. NASA-approved rotary bioreactor enhances proliferation and osteogenesis of human periodontal ligament stem cells. Stem Cells Dev. 2009;18(9):1273–82.
24. Lei X-h, Ning LN, Cao YJ, Liu S, Zhang SB, Qiu ZF, et al. NASA-approved rotary bioreactor enhances proliferation of human epidermal stem cells and supports formation of 3D epidermis-like structure. PLoS One. 2011;6(11):e26603.
25. Liu L, Wu W, Tuo X, Geng W, Zhao J, Wei J, et al. Novel strategy to engineer trachea cartilage graft with marrow mesenchymal stem cell macroaggregate and hydrolyzable scaffold. Artif Organs. 2010;34(5):426–33.
26. Lin HJ, O'Shaughnessy TJ, Kelly J, Ma W. Neural stem cell differentiation in a cell–collagen–bioreactor culture system. Dev Brain Res. 2004;153(2):163–73.
27. Sargent CY, Berguig GY, McDevitt TC. Cardiomyogenic differentiation of embryoid bodies is promoted by rotary orbital suspension culture. Tissue Eng A. 2009;15(2):331–42.
28. Cummings L, Waters S. Tissue growth in a rotating bioreactor. Part II: fluid flow and nutrient transport problems. Math Med Biol. 2007;24(2):169–208.
29. Lee P, Tran K, Chang W, Shelke NB, Kumbar SG, Yu X. Influence of chondroitin sulfate and hyaluronic acid presence in nanofibers and its alignment on the bone marrow stromal cells: cartilage regeneration. J Biomed Nanotechnol. 2014;10(8):1469–79.
30. Murphy CM, Haugh MG, O'Brien FJ. The effect of mean pore size on cell attachment, proliferation and migration in collagen–glycosaminoglycan scaffolds for bone tissue engineering. Biomaterials. 2010;31(3):461–6.
31. Valmikinathan C, et al. Novel nanofibrous spiral scaffolds for neural tissue engineering. J Neural Eng. 2008;5:422–32.
32. Evans, G., et al. Tissue engineered nerve conduits: the use of biodegradable poly-DL-lactic-co-glycolic acid (PLGA) scaffolds in peripheral nerve regeneration, in biological matrices and tissue reconstruction 1998, Springer p 225–235.
33. Wang J, Valmikinathan CM, Liu W, Laurencin CT, Yu X. Spiral-structured, nanofibrous, 3D scaffolds for bone tissue engineering. J Biomed Mater Res A. 2010;93(2):753–62.
34. Yu X, Botchwey EA, Levine EM, Pollack SR, Laurencin CT. Bioreactor-based bone tissue engineering: the influence of dynamic flow on osteoblast phenotypic expression and matrix mineralization. Proc Natl Acad Sci U S A. 2004;101(31):11203–8.
35. Freidin M, Asche S, Bargiello TA, Bennett MVL, Abrams CK. Connexin 32 increases the proliferative response of Schwann cells to neuregulin-1 (Nrg1). Proc Natl Acad Sci. 2009;106(9):3567–72.